06-3058

A Nanofibrillar Prosthetic Modified with Fibroblast Growth Factor-2 for Spinal Cord Repair

Sally Meiners[1], Suzan L. Harris[1], Roberto Delgado-Rivera[1,2], Ijaz Ahmed[1], Ashwin N. Babu[1], Ripal P. Patel[1], and David P. Crockett[3]

[1]Department of Pharmacology, UMDNJ-Robert Wood Johnson Medical School, Piscataway, NJ 08854
[2]Department of Chemistry and Chemical Biology, Rutgers University, Piscataway, NJ 08854
[3]Department of Neuroscience and Cell Biology, UMDNJ-Robert Wood Johnson Medical School, Piscataway, NJ 08854

Proofs and correspondence to:
Dr. Sally Meiners
Department of Pharmacology
UMDNJ-Robert Wood Johnson Medical School
675 Hoes Lane, Piscataway, NJ 08854
(732) 235-2890
FAX: (732) 235-4073
E-mail: meiners@umdnj.edu

06-3058

ABSTRACT

Thousands of new cases of spinal cord injury occur each year in the USA alone. However, despite recent advances, there is at present no cure for the resulting paraplegia or quadriplegia. This chapter evaluates a spinal cord prosthetic (SCP) developed in our laboratoy that is comprised of longitudinally bundled strips of nanofibers whose surfaces have been modifed with fibroblast growth factor-2 (FGF-2). The SCP is designed to be a prefabricated implant that can be grafted into the lesion site not only to provide structural but also to provide chemical cues that permit regenerating axons to cross the lesion site. For a comparative study, two separate SCPs were produced with one containing unmodified nanofibers and the other containing FGF-2-modified nanofibers. Both SCPs correctly guided regenerating axons across the injury gap created by an over-hemisection to the adult rat thoracic spinal cord and encouraged revascularization of the injury site. Neither SCP initiated glial scarring when implanted into the injured rat spinal cord. However, devices that incorporated nanofibers modified with FGF-2 encouraged more axonal regrowth and significantly better functional recovery than did devices that incorporated unmodified nanofibers as assessed using the Basso, Beattie, Bresnahan (BBB) locomotor rating scale. As such, the FGF-2-modified SCP provides a multi-faceted approach to spinal cord repair.

INTRODUCTION

This work explores the utility of electrospun nonwoven polyamide nanofibers (average fiber diameter of ~180 nm) as components of implantable prosthetics for the regeneration of axons in the lesioned spinal cord. Electrospun nanofibers were chosen because they are structurally mimetic of the basement membrane, an ultra-dense form of the extracellular matrix [Ahmed et al., 2006]. This property has created great interest in the use of nanofibers for tissue engineering applications, yet their use for *in vivo* applications is still in its early stages.

The polyamide nanofibers considered in this chapter have several important advantages for regenerative medicine strategies. As we have discussed previously [Meiners et al., 2007], they promote neuronal attachment and neurite generation [Ahmed et al., 2006] and produce no apparent cytotoxicity *in vitro* [Ahmed et al., 2006] or *in vivo* [Meiners et al., 2007]. They do not rapidly degrade, and as such, they maintain their structural integrity for several weeks *in vivo* [Meiners et al., 2007]. This is highly relevant in that a scaffold to be used for repair of spinal cord injuries must be present in the damaged spinal cord for a sufficient period of time to allow optimal axonal regeneration across the injury site. This process generally requires weeks to months depending on the position and extent of the injury. Furthermore, scaffolds composed of rapidly biodegradable materials, such as polylactate, can release acidic monomers as they break down, with negative effects on remodeling tissue [Cordewener et al., 2004]. An additional attractive attribute of nonwoven polyamide fabrics is that they are strong yet exceedingly flexible [Moeschel et al., 2002], allowing them to adapt to a variety of sizes and shapes of lesion gaps. Finally, and perhaps most importantly, recent work from our

laboratory demonstrates the promise of polyamide nanofibers in strategies for repair of the injured spinal cord [Meiners et al., 2007].

The work described in the Meiners et al. [2007] study utilized a nanofibrillar fabric comprised of randomly oriented electrospun polyamide nanofibers, itself randomly folded upon implantation into the lesioned spinal cord. This implant was associated with several promising attributes, including promotion of modest axonal regrowth with concurrent reduction of cavitation, infiltration of inflammatory cells, and glial scarring, yet it failed to orient the growth of regenerating neuronal processes. Different methodologies were considered to overcome this problem. Because neurites extend along the axis of the nanofibers [Yang et al., 2005], nanofibers with a parallel orientation would appear to be ideal for encouraging targeted axonal regeneration in the damaged spinal cord. However, aligned nanofibers exhibit considerable rigidity in comparison to randomly oriented nanofibers [Lee et al., 2005], and thus implants of aligned nanofibers may cause further damage to the delicate spinal cord tissue.

As an alternative, we developed a spinal cord prosthetic (SCP) that incorporates narrow strips of randomly oriented nanofibers that are longitudinally bundled to provide appropriate geometric cues for axonal regrowth. (See Figure 1.) The advantage of such an SCP is manifest in cases involving large injuries with extensive tissue loss. While the design of this SCP provided benefits for axonal regeneration, a large body of work suggests that the nanofibrillar SCP alone will be unlikely to promote optimal axonal regeneration and functional recovery following spinal cord injury in the absence of growth promoting chemical cues. As an example, axonal regrowth on the randomly folded nanofibrillar implant described in Meiners et al. [2007] was enhanced in the

presence of a neurite outgrowth promoting peptide identified by our research group [Meiners et al., 2001; Ahmed et al., 2006] and derived from the amino acid sequence of the extracellular matrix molecule tenascin-C.

Fibroblast growth factor-2 (FGF-2) is another growth promoting chemical cue that is perhaps an even more promising candidate for inclusion in strategies to repair spinal cord injury than the tenascin-C-derived peptide. In addition to stimulating neurite outgrowth, FGF-2 guides extending neuronal processes, promotes neuronal survival, and encourages angiogenesis [Teng et al., 1999; Webber et al., 2005; Gill et al., 2006; Heinzman et al., 2008]. The potential of FGF-2 in spinal cord injury repair is supported by ample experimental evidence. In one study, FGF-2 was expressed by adenoviral injection within glia in the dorsal spinal cord, resulting in regeneration of crushed axons within the dorsal root and significant recovery of thermal sensory function [Romero et al., 2001]. In another study, continuous intrathecal administration of soluble FGF-2 to the spinal cord following contusion injury significantly improved recovery of hindlimb function [Rabchevsky, 2000]. Our own data, presented in this chapter, demonstrate that an SCP covalently modified with FGF-2 can increase axonal regeneration and hindlimb motor functional recovery in the over-hemisected rat thoracic spinal cord in comparison to an unmodified SCP.

An additional point can be made about the significant practical advantage of utilizing immobilized FGF-2 as opposed to soluble FGF-2. FGF-2-modified nanofibers can be stored in their dry state for 6 months at 4^{o} C with retention of significant biological activity (Nur-E-Kamal et al., 2008). In contrast, soluble FGF-2 is notoriously unstable, with an approximate half-life in tissue culture media of 6-8 hours (Caldwell et

al., 2004). The stability of bound FGF-2 is a promising attribute that could lend itself to a grafting material designed to be prefabricated in bulk, trimmed to fit into a variety of defects, and ready for use as the need arises, all major advantages for its proposed future use in the clinic. The design of the FGF-2-modified SCP suggests that it would also be of benefit for applications involving repair of damage within the peripheral nervous system (PNS), as will be discussed below.

MATERIALS and METHODS

Polyamide Nanofibers. Randomly oriented polyamide (proprietary composition) nanofibers were electrospun onto aluminum foil by Donaldson Co., Inc. (Minneapolis, MN) from a blend of two polymers [$(C_{28}O_4N_4H_{47})_n$ and $(C_{27}O_{4.4}N_4H_{50})_n$]. The nanofibrillar mat was cross-linked in the presence of an acid catalyst. The nanofibers were carefully peeled off the foil and were left unmodified or were covalently modified with a proprietary polyamine polymer by Surmodics, Inc. (Eden Prairie, MN) to provide functional groups for attachment of bioactive molecules. Nanofibers and amine-modified nanofibers were then exposed to UV light for 15-30 min for sterilization. The amine-modified nanofibers were in turn covalently modified with FGF-2 under sterile conditions as we have described previously (Nur-E-Kamal et al., 2008).

Manufacture of SCPs. Strips of the unmodified or FGF-2-modified nanofibrillar fabric were cut using a Stoelting (Wood Dale, IL) tissue slicer to a width of 0.5 mm to allow ample room for axonal fasciculation and to a length of 1 cm. The strips were dipped one by one into SeaPrep® agarose (Cambrex Bioscience Rockland, Inc., Rockland, ME) (2% in dd H_2O) and stacked next to and on top of each other to result in a device ~2 mm high

and 3 mm wide when hydrated. The device was chilled at 4°C, cut into 2 mm lengths, and kept in a sterile, moist environment until implanted into the lesioned rat spinal cord as described below. SeaPrep® agarose has a gelling temperature of 8-17°C, and remains semi-liquid at room temperature. Thus it provides a liquid or semi-liquid medium at body temperature to allow for ready infiltration of cells and fasciculation of axons in between the nanofiber layers.

Surgical Procedure and Postoperative Care. All animal procedures were performed in strict accordance with institutional guidelines and approved animal protocols (Institutional Animal Care and Use Committee). The animal subjects were adult female Sprague Dawley rats (250-260 g) (Hilltop Laboratories Animals, Inc., Scottsdale, PA). The rats were divided into three groups of five rats each. The first group received a multi-layered implant that incorporated unmodified nanofibers, while the second group received a multi-layered implant that incorporated FGF-2-modified nanofibers. The third group received an injury but no implant (injury only control group).

The implantation procedure was done as follows. Rats were anesthetized using isoflurane administered in a fume hood followed by ketamine/xylazine (75 mg/kg + 10 mg/kg, intraperitoneal (IP)). They were also given buprenorphine (0.05 mg/kg, delivered subcutaneously) before surgery for post-operative pain. In addition, bupivocaine was used as a topical anesthetic. Using aseptic rodent surgery techniques, an incision was made over the thoracic region of the spinal cord. A double laminectomy was performed at thoracic level 8-9. Irridectomy scissors were used to make a transverse cut 2 mm deep to the dorsal columns of the spinal cord. Another transverse cut was made 2 mm caudal to the first, and the tissue in between was removed with scissors to a depth of 2 mm.

After creating the lesion, a sterile SCP (unmodified or modified with FGF-2) made on the prior day was placed in the cavity with the 2 mm long axis longitudinal to the spinal cord. Control animals were subjected to the identical surgery but received no SCP. The musculature was sutured with silk, and the skin was closed with stainless steel surgical clips.

Immediately post-surgery, rats were placed in a cage set on top of a heating pad set to 37°C until consciousness was regained. (Ambient cage temperature was no more than 85°F.) They were provided with means to move away from the heating pad once they were awake. Animals were monitored at least every 15 minutes until anesthetic recovery. They were then monitored 3 times daily during the first 4-7 days post-surgery for any signs of pain or infections and 1-2 times daily on weekdays and at least once a day on weekends thereafter so that any health problems could be observed as soon as possible. The rats were housed two to a cage and were provided with red transparent plastic tubes (3 inches in diameter and 6 inches long) for nesting once they regained enough rear hindlimb mobility to allow maneuvering in and out of the tube. This generally did not occur for at least 7 days post surgery.

Sterile lactated Ringer's solution was administered subcutaneously post-surgery 3 times daily for a total of 15 ml per day until the animals were observed to be drinking on their own. Apple slices (sometimes dipped in peanut +butter) were also provided to stimulate the appetite and to provide extra hydration for 4-5 days. In addition, the rats were given analgesics (buprenorphine, 0.05 mg/kg delivered subcutaneously) and antibiotics (enrofloxacin (Baytil), 5 mg/kg delivered subcutaneously) immediately after surgery. Buprenorphine was given 2-3 times daily for 1-2 days, and enrofloxacin was

given 2 times daily for at least 3 days. Bladders were evacuated 3 times daily until autonomic bladder function was restored (usually 4-7 days). Surgical clips were removed after 2 weeks.

Functional Assessment. Recovery of hindlimb locomotor function was assessed on a daily basis for 3 weeks using the 21 point Basso, Beattie, Bresnahan (BBB) locomotor rating scale to evaluate open field locomotion (Basso et al., 1995). The BBB scale has the advantage of providing an assessment tool spanning complete paralysis to normal hindlimb locomotion by rating a wide variety of parameters observed during recovery of function. Although this scale was designed for assessment of open-field locomotion recovery after contusion injuries, it has been successfully applied to the assessment of over-hemisection injuries as well (Deumens et al., 2006).

Immunohistochemistry. Following postoperative periods of 3 weeks, animals were re-anesthetized using isoflurane followed by ketamine/xylazine (75 mg/kg + 10 mg/kg, IP) and perfused transcardially first with 0.9% NaCl in 0.1 M sodium phosphate buffer containing 50 U/ml heparin (Sigma Chemical Co., St. Louis, MO) and then with 0.1 M sodium phosphate buffer containing 4% paraformaldehyde fixative. Spinal cords were removed, and sagittal sections were cut on a cryostat to a thickness of 20 μm. Sections were mounted on plus (+) gold glass slides (Fisher Scientific, Inc., Hampton, NH). They were then immunolabeled for axons with a mouse monoclonal antibody against neurofilament-M (Millipore Corporation, Billerica, MA) (1:500 dilution overnight at room temperature) and a CY3-conjugated goat anti-mouse secondary antibody (1:500 dilution for 1 hour at room temperature). Some sections were double labeled as described with the antibody against neurofilament-M followed by a rabbit polyclonal

antibody against calcitonin gene-related peptide (CGRP) (Millipore (formerly Chemicon), Billerica, MA) (1:5,000 dilution overnight at room temperature) and a donkey anti-rabbit secondary antibody (1:300 dilution for 1 hour at room temperature).

Other sections were stained with a rabbit polyclonal antibody against collagen IV (Research Diagnostics Inc., Division of Fitzgerald Industries, Concord, MA) (1:500 dilution overnight at room temperature) and a CY2-conjugated donkey anti-rabbit secondary antibody (1:300 dilution for 1 hour at room temperature) to detect blood vessels and Schwann cells; or with a rabbit polyclonal antibody against glial fibrillary acidic protein (GFAP) (Dako Inc., Carpinteria, CA) (1:500 dilution overnight at room temperature) and a CY2-conjugated donkey anti-rabbit secondary antibody (1:300 dilution for 1 hour at room temperature) to detect astrocytes. At least 15-20 sections per spinal cord were examined. Both secondary antibodies were from Jackson Laboratories (West Grove, PA), and all antibodies were diluted in phosphate buffered saline (PBS) containing 0.3% Triton X-100. Images of the labeled spinal cord sections were captured using a Zeiss Axioplan microscope (Carl Zeiss, Inc., Maplegrove, MN) equipped with an epi-fluorescence illuminator and axiovision software.

RESULTS and DISCUSSION

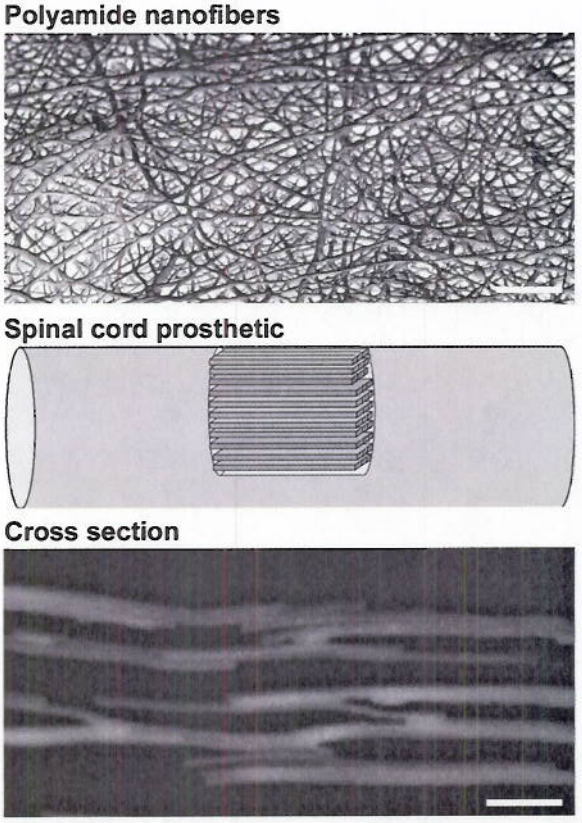

Figure 1. Manufacture of the SCP. (Top) Nonwoven fabric of electrospun nanofibrillar fabric used to manufacture the SCP. Scale bar, 5 μm. **(Middle)** Schematic diagram of the SCP within the spinal cord. **(Bottom)** Epi-fluorescence image showing a cross section through an unmodified SCP prior to implantation into the spinal cord. The nanofibrillar strips can be visualized due to their low level of autofluorescence. Note the conduits resulting from the stacking of the strips next to and on top of each other. Scale bar, 100 μm.

Nanofibrillar SCPs. Electrospun polyamide nanofibers used for the manufacture of the SCP are shown in Figure 1 (top). The nonwoven nanofibrillar fabric was ~ 2 μm thick and comprised of nanofibers with a median diameter of 180 nm. The nanofibers were interspersed with pores with diameters ranging from 100-800 nm (Schindler et al., 2005). A schematic diagram of the SCP is illustrated in Figure 1 (middle). The SCP was comprised of a bundle of nanofibrillar strips (unmodified or FGF-2-modified) 0.5 mm wide x 2 mm long bundled together with low gelling temperature agarose. Each device was approximately 6 nanofibrillar strips wide and 45 nanofibrillar strips high and was implanted into the over-hemisected spinal cord with the 2 mm long axis longitudinal to the spinal cord. A cross section through an SCP made on the day prior to implantation and stored at 4°C until use (Figure 1, bottom) revealed that the nanofibrillar strips within the device resembled a stack of bricks laid in a staggered

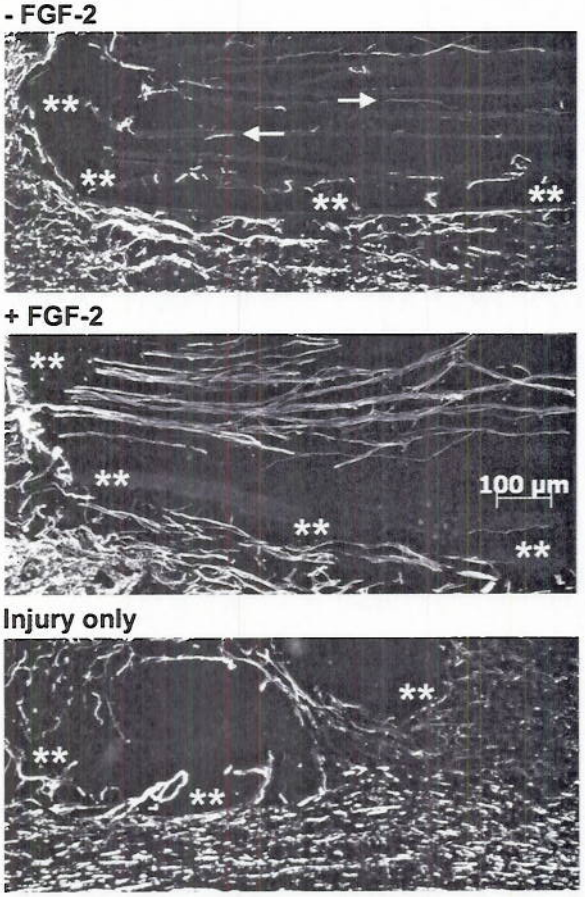

Figure 2. Axonal elongation onto SCPs in the injured spinal cord. Rostral is to the left. Immunostaining was performed using an antibody against neurofilament-M. Neurofilament M-labeled axons were detected using epi-fluorescence microscopy. Nanofiber strips are faintly visible due to autofluorescence. The lesion edge is marked with asterisks. **(Top)** Axons were observed within the SCP containing bundled strips of unmodified nanofibers 3 weeks after injury. An axon apparently growing on the surface of a nanofibrillar strip is marked with an arrow pointing to the left, whereas an axon growing in between nanofibrillar strips is marked with an arrow pointing to the right. **(Middle)** More axons were seen within the FGF-2-modified prosthetic. A large degree of fasciculation was observed. **(Bottom)** Some axons were observed in the lesion site in injury only controls, but they grew with no particular orientation.

pattern, providing both surface area for cellular growth and agarose filled conduits in between the nanofibrillar layers.

Axonal Regrowth on Unmodified and FGF-2-Modified SCPs.

Immunohistochemical techniques were employed utilizing epi-fluorescence microscopy and an antibody against neurofilament-M, a general axonal marker, to visualize axons 3 weeks after injury (Figure 2). The nanofibrillar strips within the implanted SCPs were detectable as a consequence of their low level of autofluorescence. Some axons were observed within SCPs that incorporated strips of the unmodified polyamide nanofibrillar fabric (Figure 2, top). The axons were observed both associated with the nanofibrillar surface (left-hand arrow) and in between the nanofibrillar layers (right-hand arrow), although it is possible that the latter were growing on nanofibers out of the focal plane of the section or on cells such as Schwann cells (see below) that were themselves associated with nanofibers.

More, and apparently longer, neurofilament-M-labeled axons were observed within SCPs that incorporated nanofibrillar strips covalently modified with FGF-2 in comparison to SCPs that incorporated unmodified nanofibrillar strips (Figure 2, middle). The axons grew with the correct longitudinal orientation within both types of SCP, while agarose alone provided no guidance to the extending processes (data not shown). No axons were observed within the SCPs immediately after injury, indicating that the observed axons were regenerating as opposed to axons spared in the lesion process (data not shown). Some axons were observed in the lesion site in injury only control animals, but these were for the most part short, fragmented, and randomly oriented (Figure 2, bottom).

Inspection of axons at higher magnification revealed fasciculated neuronal processes within both the unmodified (Figure 3, top) and FGF-2-modified (Figure 3, middle, bottom) SCPs. However, axons within the FGF-2-modified devices demonstrated a more

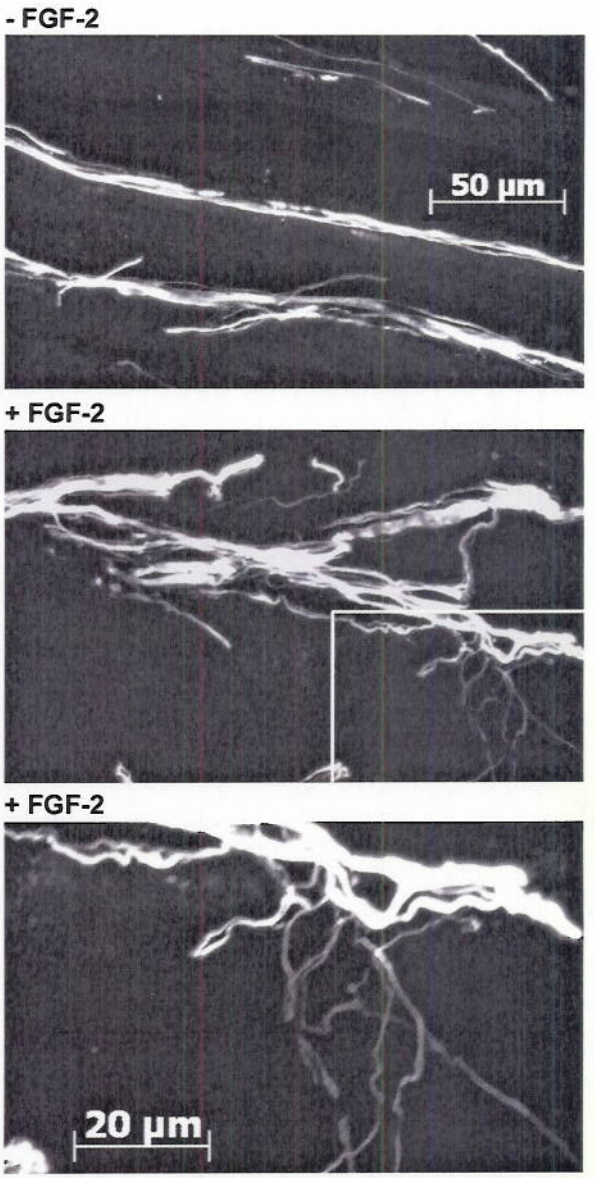

Figure 3. Morphology of regenerating axons. Immunostaining was performed using an antibody against neurofilament-M. Axons were detected using epi-fluorescence microscopy. **(Top)** Axons within unmodified SCPs demonstrated relatively little branching. **(Middle)** Axons within FGF-2-modifed SCPs had a more complex morphology, with abundant branching. The boxed area is enlarged **(bottom)** to highlight the ramified structure.

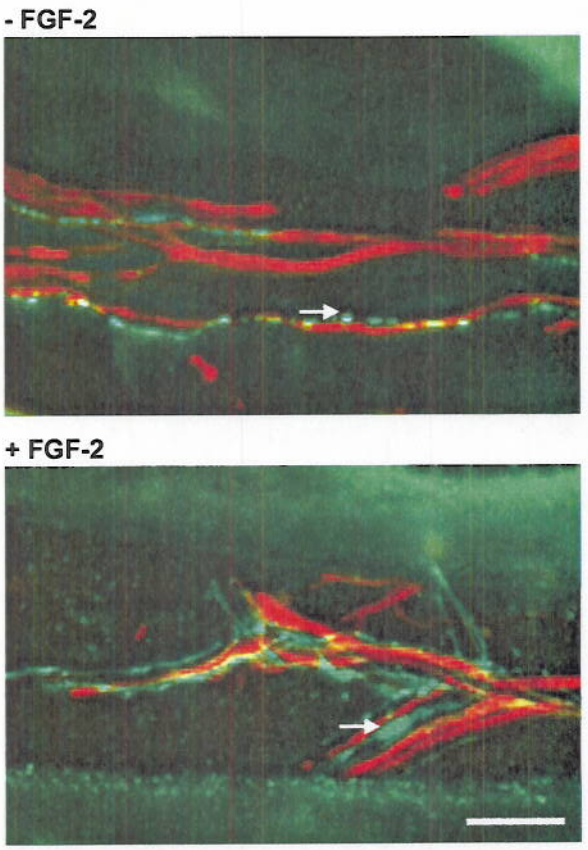

Figure 4. Boutons en passant. Immunostaining was performed using antibodies against neurofilament-M (red) and CGRP (green). Axons were detected using epi-fluorescence microscopy. CGRP-labeled axons within unmodified **(top)** and FGF-2-modified **(bottom)** SCPs demonstrated localized swellings (arrows) along their length that were characteristic of boutons en passant. The nanofibrillar layers in the bottom panel autofluoresced green. Scale bar, 25 μm.

complicated morphology, with an increase in axon branching. In another study, Szbenyi et al. [2001)] demonstrated that local application of FGF-2 (presented as FGF-2-coated polystyrene microspheres that were first covalently coupled to heparin) promoted branching *in vitro* of embryonic sensory motor cortical neuronal axons. Distal regions of the axon, in particular the growth cone, were more likely to respond to the branch-inducing effects of the growth factor, suggesting that FGF-2 in target regions of the developing cortex may influence target recognition and synapse formation through arborization of interstitial collaterals. In a similar fashion, FGF-2 immobilized to nanofibers in the injured spinal cord may enhance neuronal plasticity and synapse formation may encourage ramification of regenerating axons.

Some sections were double labeled using antibodies against neurofilament-M (red) as well as CGRP (green) (Figure 4). CGRP is a marker for primary peptidergic sensory neurons [Xu et al., 1999; Jones et al., 2001], although it can also be expressed in motor neurons [Ramer et al., 2003]. Evidence for synapse formation was observed in the

form of swellings (arrows), or boutons, along the length of the CGRP-labeled processes in close proximity to the neurofilament-M-labeled axons. These "boutons en passant" were seen within both unmodified and FGF-2-modified SCPs. Examination of the sections using rhodamine (CY3) and fluorescein (CY2) optics revealed that many of the CGRP-labeled axons did not appear to be labeled with the antibody against neurofilament-M (data not shown). This observation is in agreement with that of Petruska et al. [2002] that some, but not all, CGRP-positive dorsal root ganglion neurons express neurofilament-M.

Recovery of Hindlimb Motor Function. Results from the axon labeling studies were most encouraging in regard to the regenerative performance of the FGF-2-modified SCP. However, given the difficulties inherent in quantifying axonal regrowth by immunohistochemical methods, functional assays provide the best means for evaluation of an intervention to facilitate spinal cord repair. Indeed, even data indicative of boutons en passant (Figure 4), or data from tract tracing experiments demonstrating the growth of axons off the implant and into the caudal spinal cord [Teng et al., 2002], do not provide information about restoration of *functional* connections. Therefore, BBB locomotor scores were determined for rats that received an unmodified SCP, an FGF-2-modified SCP, or an identical over-hemisection lesion with no implant.

BBB scores were significantly improved as early as 3-4 days following injury for rats that received an FGF-2-modified SCP in comparison to an unmodified SCP (Figure 5). Both groups continued to improve on the BBB rating scale throughout the 21 days of the experiment, but the FGF-2-modified SCP group showed significant improvements over the unmodified SCP group at the majority of the time points. Because the enhanced

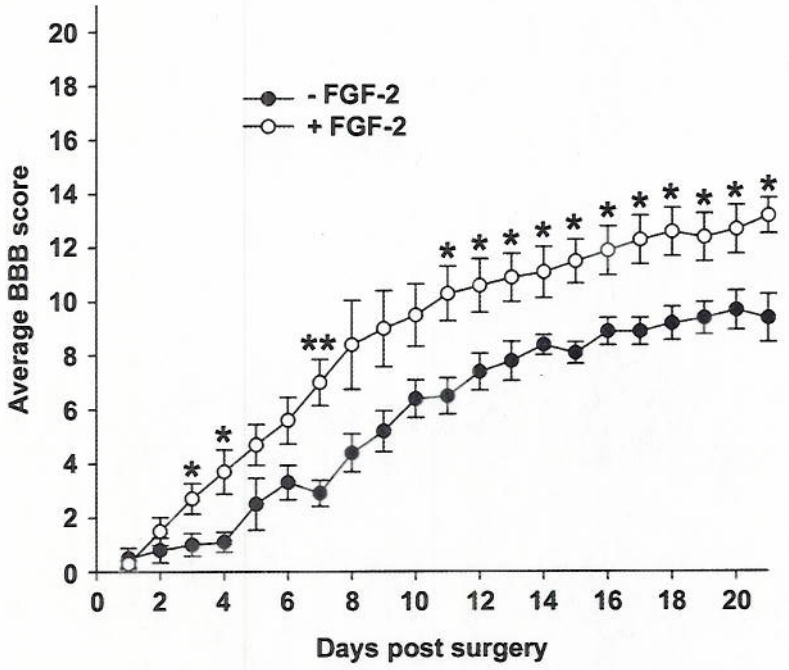

Figure 5. Hindlimb functional assessment with the BBB locomotor rating scale. Curves represent the mean +/- the standard error of the mean (n = 5 rats per group). Animals were tested daily for 3 weeks. Rats that received an FGF-2-modified SCP **(white circles)** showed enhanced functional recovery in comparison to rats that received an unmodified SCP **(black circles)**. Single asterisks denote significant differences between the two groups at each time point with $p < 0.05$; double asterisks denote significant differences with $p < 0.01$ (Student's T-test).

impact of the growth factor-modified device was first noted at such an early time point, before axonal regeneration could reasonably be expected to occur, it is likely that the FGF-2-modified SCP had an anti-lesion and/or a neuroprotective effect in addition to or instead of an axonal regeneration effect.

On the other hand, the degree of functional recovery afforded by the unmodified SCP did not vary significantly from the extent of spontaneous functional recovery observed for injury only control animals (data not shown). The spontaneous recovery for the latter was probably due to lingering function of the central pattern generator for locomotion present in rats [Babu and Namasivayam, 2008]. This result was surprising given clear evidence that the nanofibrillar conduits provided guidance for regenerating neuronal processes (Figure 2) and in turn suggests that some other property of the implant impeded optimal functional recovery in spite of the oriented regrowth.

Inspection of the entire lesion site revealed evidence of a fluid-filled cyst at the caudal end of the implant. Cyst formation occurred to varying degrees and was observed

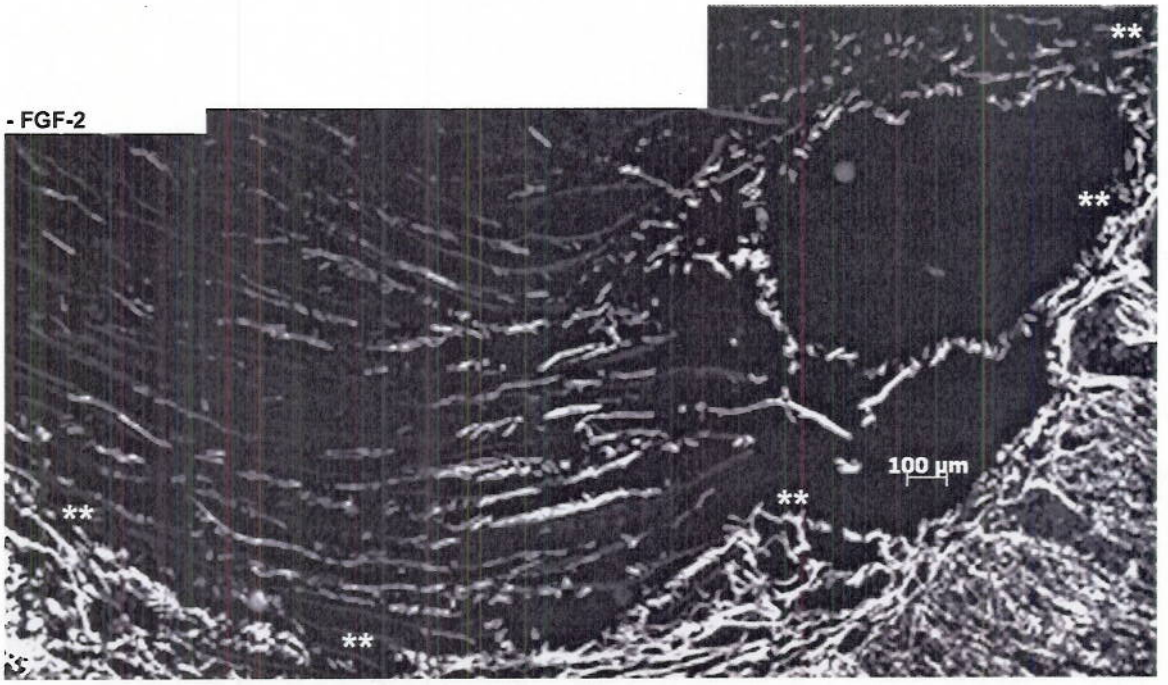

Figure 6. Evidence for buildup of pressure within the SCP. Rostral is to the left. Immunostaining was performed using an antibody against neurofilament-M. Axons within an unmodified SCP were detected using epi-fluorescence microscopy. A large cavity suggestive of a fluid-filled cyst was observed at the caudal end of the device.

for both unmodified (Figure 6) and FGF-2-modified SCPs. Importantly, somewhat more regrowth within the unmodified SCP is visible in the section shown in Figure 6 in comparison to the section shown in Figure 2, again underscoring the vagaries of immunohistochemical assessment of axonal regeneration in comparison to behavioral assessment of functional recovery. The probable cause of the cyst formation was an impediment to the flow of cerebral spinal fluid (CSF) due to the viscosity of the agarose. Therefore, it seems likely that employing a more porous medium to separate the nanofibrillar layers would result in an SCP that allows better axonal regrowth at and beyond the distal end of the implant, with additional behavioral benefits.

We previously discussed a multi-layer nanofibrillar fabric engineered by Donaldson Co., Inc. for possible application in spinal cord injury strategies [Meiners et al., 2007]. This fabric incorporated individual nanofibrillar layers that were separated by

beads. While this design would be expected to aid in the free flow of CSF, the nanofibrillar layers were only separated from each other by about 10 μm. On the other hand, a separation of 50-200 μm is optimal to allow sufficient room for cellular growth and revascularization [Stokols et al., 2004; Yu et al., 2005], necessitating larger beads or a different kind of spacer. Other possibilities for separation of nanofibrillar layers with requisite porosity and spacing include templated agarose scaffolds containing linear channels [Stokols et al., 2006] or cross-linked hydrogels [Pike et al., 2006].

Revascularization and Infiltration of Schwann Cells. Immunostaining with an antibody against collagen IV was done to evaluate ingrowth of blood vessels and infiltration of Schwann cells, both of which express this basement membrane protein following spinal cord injury [Klapka & Werner Muller, 2006; Buss et al., 2007]. An abundance of collagen IV-positive blood vessels (BV) was observed within both unmodified (data not shown) and FGF-2-modified SCPs (Figure 7). This is important because revascularization is vital and necessary for the ultimate efficacy of the SCP. Blood vessels supply nutrients to regenerating tissues and precede axons in successful models of regeneration [Loy et al., 2002].

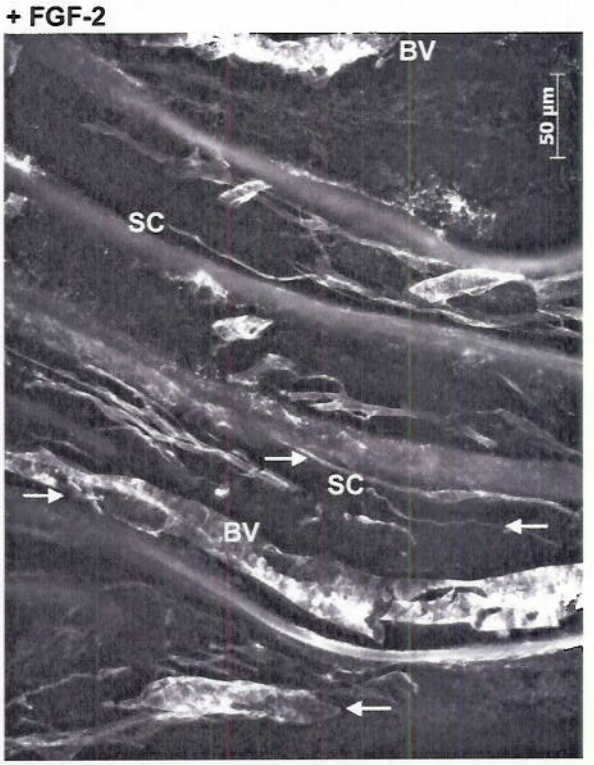

Figure 7. Re-vascularization within an FGF-2-modified SCP. Rostral is to the left. Immunostaining was performed using an antibody against collagen IV. Blood vessels (BV) and Schwann cells (SC) were detected within an FGF-2-modified SCP using epi-fluorescence microscopy. Blood vessels and Schwann cells appeared to grow both on the surface of the nanofibrillar layers (left-hand arrows) and in the agarose in between the layers (right-hand arrows).

Collagen IV-positive cells with the characteristic bipolar morphology of Schwann cells (SC) were also observed within unmodified (no shown) and FGF-2-modified SCPs (Figure 7). These cells could be differentiated from blood vessels by their smaller size as well as by their morphology. Thus it is likely that the Schwann cells, in addition to the engineered components of the SCP, encouraged axonal regrowth. Indeed, as observed for cellular relationships within peripheral nerve implants [Kim et al., 2008], axons were generally observed in close proximity to the Schwann cells (data not shown). Finally, as seen for axons (Figure 2), blood vessels and Schwann cells appeared to be associated both with the nanofibrillar surface (right-hand arrows) and the agarose component of the SCP (left-hand arrows). Since FGF-2 is an angiogenic factor in the spinal cord [Hayashi et al., 1999] and furthermore promotes proliferation of Schwann cells [Shen et al., 2008], incorporation of FGF-2 into the agarose (or other spacer constituent employed) as well as onto the nanofibers may prove beneficial for the repair process.

Glial Scarring. Astrocytes, generally regarded as permissive for neuronal growth during development of the brain and spinal cord, can become reactive following brain or spinal cord injury and contribute to scar formation and regenerative failure [McLeon et al., 1991; Davies et al., 2004]. GFAP immunostaining followed by epi-fluorescence microscopy was therefore performed to visualize both reactive and non-reactive astrocytes. Reactive astrocytes, characterized by up-regulated GFAP and a hypertrophied morphology, were observed for injury only controls at the lesion edge (Figure 8, right), whereas only non-reactive astrocytes were observed at the lesion edge for animals that received an unmodified SCP (Figure 8, left) or an FGF-2-modified SCP (Figure 8, middle). However, non-reactive astrocytes were not observed within the device itself.

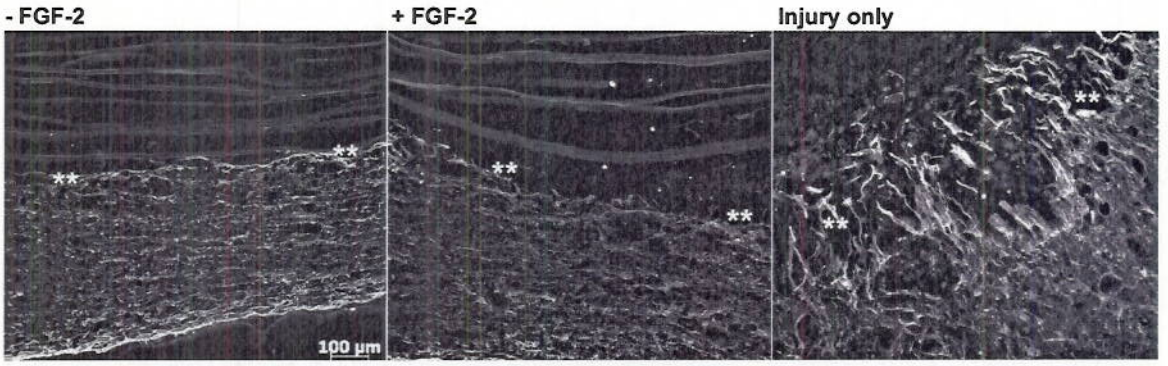

Figure 8. Exclusion of reactive astrocytes by SCPs. Rostral is to the left. Immunostaining was performed using an antibody against GFAP 3 weeks after injury. GFAP-labeled astrocytes were detected using epi-fluorescence microscopy. The lesion edge is marked with asterisks. Non-reactive astrocytes were observed within the spinal cord tissue distal to unmodified **(left)** and FGF-2-modified **(middle)** SCPs but were largely absent from the SCPs themselves. No glial scarring was observed. In contrast, reactive astrocytes were observed migrating from the lesion edge into the lesion center in injury only controls **(right)**.

Why this should be is unclear since astrocytes readily grow on unmodified and FGF-2-modified nanofibrillar matrices *in vitro* (Nur-E-Kamal et al., 2008) and on nanofibers removed from the lesioned spinal cord 3 weeks after implantation (data not shown). While lack of scarring is a crucial feature for a successful implant for tissue engineering in the central nervous system (CNS), the presence of non-reactive astrocytes would almost assuredly encourage more robust axonal regeneration and recovery of function than that currently observed.

In support of this premise, astrocytes generated from glial-restricted precursor cells promoted vigorous axonal regeneration into and beyond the lesion site when transplanted into dorsal column spinal cord injuries in adult rats [Davies et al., 2006]. Significant improvements in locomotor functional recovery as assessed by grid-walk analysis were also documented. Importantly, astrocytes grown on FGF-2-modified nanofibers become more supportive of neuronal growth when co-cultured with an overlay of neurons in comparison to their counterparts grown on more traditional glass or plastic surfaces (unpublished data). These results suggest that polyamide nanofibers may provide

an ideal scaffolding material for the implantation of exogenous non-reactive astrocytes or astrocytic stem cells into the damaged spinal cord.

Like astrocytes, infiltrating (Figure 7) and transplanted Schwann cells also promote axonal growth from spinal cord neurons and are generally regarded as permissive for the regeneration process [Bunge, 2008]. However, an advantage of astrocytes over Schwann cells is that they are endogenous to the CNS, and an implant containing astrocytes may create less of a demarcation between "self" and implant, in particular in cases where the implant does not provoke scarring in the distal tissue. Hence axons may be more prone to grow through an implant and to exit at the distal end into the spinal cord tissue in the case of an implant containing astrocytes as opposed to one pre-loaded with Schwann cells.

Other Applications. During the course of our investigations, a similar implant design for PNS regeneration was reported by Kim et al. [2008]. In this study, nanofibrillar strips comprised of randomly oriented or aligned poly (acrylonitrile-*co*-methylacrylate) nanofibers prepared by electrospinning were stacked inside a polysulfonene nerve conduit. No agarose or other spacer was necessary because the nanofibrillar strips were constrained within the nerve by the conduit. The nanofibrillar filled conduits were used to bridge a 17 mm long gap in the transected tibial nerve of adult rats. Significantly more axons regenerated through the conduits that incorporated strips of aligned nanofibers in comparison to conduits that incorporated strips of randomly oriented nanofibers, with enhanced behavioral results. The addition of growth factors to the nanofibers was not evaluated in this study. It is likely that the FGF-2-modified SCP described in this chapter could be modified to encourage PNS as well as CNS regeneration, and further, that the

mechanical stiffness of aligned polyamide nanofibers would not be a limitation in large peripheral nerves such as tibial and sciatic nerves but would in fact improve the regenerative capacity of the SCP.

CONCLUSION

An SCP comprised of longitudinally bundled strips of an electrospun, randomly oriented polyamide nanofibrillar fabric that were separated with agarose encouraged guided axonal regrowth through the implant. This property and concomitant behavioral outcomes were improved by the addition of FGF-2. Both types of SCP were permeated by blood vessels and Schwann cells, and neither type promoted glial scarring. On the other hand, quiescent astrocytes failed to populate the SCPs, and cystic cavities were frequently observed at the caudal end of the implant. In conclusion, the FGF-2-modified nanofibrillar SCP is a promising prototype for inclusion in strategies to repair spinal cord injury, but further improvements are warranted.

ACKNOWLEDGEMENTS

This work was supported by New Jersey Commission on Spinal Cord Research Grant 06A-007-SCR1 to S.M. R.D.-R. gratefully acknowledges the Rutgers-National Science Foundation Integrative Graduate Education and Research Traineeship (IGERT) program on Integratively Engineered Biointerfaces.

REFERENCES

Ahmed, I., Liu, H.-Y., Mamiya, P.C., Ponery, A.S., Babu, A.N., Weik, T., Schindler, M., & Meiners, S. (2006). Three-dimensional nanofibrillar surfaces covalently modified with tenascin-C-derived peptides enhance neuronal growth *in vitro*. J. Biomed. Mater. Res. A, 76, 851-860.

Babu, R.S. & Namasivayam, A. (2008) Recovery of bipedal locomotion in bonnet macaques after spinal cord injury: footprint analysis. Synapse, 62, 432-447.

Basso, D.M., Beattie, M.S., & Bresnahan, J.C. (1995). A sensitive and reliable locomotor rating scale for open field testing in rats. J. Neurotrauma, 12, 1-21.

Bunge, M.B. (2008) Novel combination strategies to repair the injured mammalian spinal cord. J. Spinal Cord Med., 31, 262-269.

Buss, A., Pech, K., Kakulas, B.A., Martin, D., Schoenen, J., Noth, J., & Brook, G.A. (2007) Growth-modulating molecules are associated with invading Schwann cells and not astrocytes in human traumatic spinal cord injury. Brain, 130, 940-953.

Cordewener, F.W., van Geffen, M.F., Joziasse, C.A.P.S.J.P., Bos, R.R.M., Rozema, F.R., & Pennings, A.J. (2000). Cytotoxicity of poly(96L/4D-lactide): the influence of degradation and sterilization. Biomaterials, 21, 2433-2442.

Davies, J.E., Huang, C., Proschel, C., Noble, M., Mayer-Proschel, M., & Davies, S.J. 92006) Astrocytes derived from glial-restricted precursors promote spinal cord repair. J. Biol., 5, article 7.

Davies, J.E., Tang, X., Denning, J.W., Archibald, S.J., & Davies, S.J. (2004) Decorin suppresses neurocan, brevican, phosphacan and NG2 expression and promotes

axon growth across adult rat spinal cord injuries. Eur. J. Neurosci., 19, 1226-1242.

Deumens, R., Koopmans, G.C., Honig, W.M., Maquet, V., Jerome, R., Steinbusch, H.W., & Joosten, E.A. (2006). Limitations in transplantation of astroglia-biomatrix bridges to stimulate corticospinal axon regrowth across large lesion gaps. Neurosci. Lett., 400, 208-212.

Gill, J.C. & Tsai, P.-S. (2006). Expression of a dominant negative FGF receptor in developing GNRH1 neurons disrupts axon outgrowth and targeting to the median eminence. Biol. Repro., 74, 463-472.

Hayashi, T., Sakurai, M., Abe, K., Sadahiro, M., Tabayashi, K., & Itoyama, I. (1999) Expression of angiogenic factors in rabbit spinal cord after transient ischaemia. Neuropathol. Appl. Neurobiol., 25, 63-71.

Heinzman, J.N., Brower, S.L., & Bush, J.E. (2008). Comparison of angiogenesis-related factor expression in primary tumors under normal and hypoxic growth conditions. Cancer Cell Int., e-pub ahead of print.

Jones, L.L., Oudega, M., Bunge, M.B., & Tusynski MH (2001) Neurotrophic factors, cellular bridges and gene therapy for spinal cord injury. J. Physiol., 533, 83-89.

Kim, Y.-t., Haftel, V.K., Kumar, S., & Bellamkonda, R.V. (2008) The role of aligned polymer fiber-based constructs in the bridging of long peripheral nerve gaps. Biomaterials, 29, 3117-3127.

Lee, C.H., Shin, H.J., Cho, I.H., Kang, Y.-M., Kim, I.A., Park, K.-D., Shin, J.-W. (2005). Nanofiber alignment and direction of mechanical strain affect the ECM production of human ACL fibroblast. Biomaterials, 26, 1261-1270.

Loy, D.N., Crawford, C.H., Darnall, J.B., Burke, D.A., Onifer, S.M., & Whittemore, S.R. (2002) Temporal progression of angiogenesis and basal lamina deposition after contusive spinal cord injury in the adult rat. J. Comp. Neurol., 445, 308-324.

Meiners, S., Ahmed, I., Ponery, A.S., Amor, N., Harris, S.L., Ayres, V., Fan, Y., Chen, Q., Delgado-Rivera, R., & Babu, A.N. (2007). Engineering electrospun nanofibers for spinal cord repair: A discussion. Polymer Internat., 56, 1340-1348.

Klapka, N. & Werner Muller, H. (2006) Collagen matrix in spinal cord injury. J. Neurotrauma, 23, 422-435.

McKeon, R.J., Schreiber, R.C., Rudge, J.S., & Silver, J. (1991) Reduction of neurite outgrowth in a model of glial scarring following CNS injury is correlated with the expression of inhibitory molecules on reactive astrocytes. J. Neurosci., 11, 3398-3411.

Moeschel, K., Nouaimi, M., Steinbrenner, C., & Bisswanger, H. (2002). Immobilization of thermolysin to polyamide nonwoven materials. Biotech. Bioengineer., 82, 190-199.

Nur-E-Kamal, A., Ahmed, I., Kamal, J., Babu, A.N., Schindler, M., & Meiners, S. (2008). Covalently attached FGF-2 to three-dimensional polyamide nanofibrillar surfaces demonstrates enhanced biological stability and activity. Mol. Cell. Biochem., 309,157–166.

Petruska, J.C., Napaporn, J., Johnson, R.D., & Cooper, B.Y. (2002) Chemical responsiveness and histochemical phenotype of electrophysiologically classified cells of the adult rat dorsal root ganglion. Neuroscience, 115, 15-30.

Pike, D.B., Cai, S., Pomraning, P.R., Firpo, M.A., Fisher, R.J., Shu, X.Z., Prestwich, G.D., & Peattie, R.A. (2006) Heparin-regulated release of growth factors in vitro

and angiogenic response in vivo to implanted hyaluronan hydrogels containing VEGF and bFGF. Biomaterials, 27, 5242-5251.

Rabchevsky, A.G., Fugaccia, I., Turner, A.F., Blades, D.A., Mattson, M.P., & Scheff, S.W. (2000). Basic fibroblast growth factor (bFGF) enhances functional recovery following severe spinal cord injury to the rat. Exp. Neurol., 164, 280-291.

Ramer, M.S., Bradbury, E.J., Michael, G.J., Lever, I.J., & McMahon, S.B. (2003) Glial cell line-derived neurotrophic factor increases calcitonin gene-related peptide immunoreactivity in sensory and motoneurons in vivo. Eur. J. Neurosci., 18, 2713-2721.

Romero, M.I., Rangappa, N., Garry, M.G., & Smith, G.M. (2001). Functional regeneration of chronically injured sensory afferents into adult spinal cord after neurotrophin gene therapy. J. Neurosci., 21, 8408-8416.

Schindler, M., Ahmed, I., Kamal, J., Nur-e-Kamal, A., Grafe, T.H., Chung, H.Y., & Meiners, S. (2005). Three dimensional nanofibrillar surfaces promote *in vivo*-like organization and morphogenesis for cells in culture. Biomaterials, 26, 5624-5631.

Shen, B., Pei, F.X., Duan, H., Chen, J., & Mu, J.X. (2008) Preparation and in vitro activity of controlled release microspheres incorporating bFGF. Chin. J. Traumatol.,11, 22-27.

Stokols, S., Sakamoto, J., Breckon, C., Holt, T., Weiss, J., & Tuszynski, M.H. (2006) Templated agarose scaffolds support linear axonal regeneration. Tissue Eng., 12, 2777-2787.

Stokols, S. & Tuszynski, M.H. (2004) The fabrication and characterization of linearly oriented nerve guidance scaffolds for spinal cord injury. Biomaterials, 25, 5839-5846.

Szebenyi, G., dent, E.W., Callaway, J.L., Seys, C., Lueth, H., & Kalil, K. (2001) Figroblast growth factor-2 promotes axon branching of cortical neurons by influencing morphology and behavior of the primary growth cone. J. Neurosci., 21, 3932-3941.

Teng, Y.D., Mocchetti, I., Taveira-DaSilva, A.M., Gillis, R.A., & Wrathall, J.R. (1999). Basic fibroblast growth factor increases long-term survival of spinal motor neurons and improves respiratory function after experimental spinal cord injury. J. Neurosci., 19, 7037-7047.

Teng, Y.D., Lavik, E.B., Qu, X., Park, K.I., Ourednik, J., Zurakowski, D., Langer, R., & Snyder, E.Y. (2002) Functional recovery following traumatic spinal cord injury mediated by a unique polymer scaffold seeded with neural stem cells. Proc. Natl. Acad. Sci. U.S.A., 99, 3024-3029.

Webber, C.A., Chen, Y.Y., Hehr, C.L., Johnston, J., & McFarlane S (2005). Multiple signaling pathways regulate FGF-2-induced retinal ganglion cell neurite extension and growth cone guidance. Mol. Cell. Neurosci., 30, 37-47.

Xu, X.M., Zhang, S.X., Li, H., Aebischer, P., & Bunge, M.B. (1999) Regrowth of axons into the distal spinal cord through a Schwann-cell-seeded mini-channel implanted into hemisected adult rat spinal cord. Eur. J. Neurosci. 11, 1723-1740.

Yang, F., Murugan, R., Wang, S., & Ramakrishna, S. (2005). Electrospinning of nano/micro scale poly(L-lactic acid) aligned fibers and their potential in neural tissue engineering. Biomaterials, 26, 2603-2610.

Yu, T.T. & Shoicet, M.S. (2005) Guided cell adhesion and outgrowth in peptide-modified channels for neural tissue engineering. Biomaterials, 26, 1507-1514.

Reviewed by Dr. Bonnie Firestein-Miller, Department of Cell Biology and Neuroscience, Rutgers University, Piscataway, New Jersey, USA, and Dr. Melvin Schindler, Nanonoculture LLC, Piscataway, New Jersey, USA.

FIGURE LEGENDS

Figure 1. Manufacture of the SCP. (Top) Nonwoven fabric of electrospun nanofibrillar fabric used to manufacture the SCP. Scale bar, 5 μm. **(Middle)** Schematic diagram of the SCP within the spinal cord. **(Bottom)** Epi-fluorescent image showing a cross section through an unmodified SCP prior to implantation into the spinal cord. The nanofibrillar strips can be visualized due to their low level of autofluorescence. Note the conduits resulting from the stacking of the strips next to and on top of each other. Scale bar, 100 μm.

Figure 2. Axonal elongation onto SCPs in the injured spinal cord. Rostral is to the left. Immunostaining was performed using an antibody against neurofilament-M. Neurofilament M-labeled axons were detected using epi-fluorescence microscopy. Nanofiber strips are faintly visible due to autofluorescence. The lesion edge is marked with asterisks. **(Top)** Axons were observed within the SCP containing bundled strips of unmodified nanofibers 3 weeks after injury. An axon apparently growing on the surface of a nanofibrillar strip is marked with a left-hand arrow, whereas an axon growing in between nanofibrillar strips is marked with a right-hand arrow. **(Middle)** More axons were seen within the FGF-2-modified prosthetic. A large degree of fasciculation was observed. **(Bottom)** Some axons were observed in the lesion site in injury only controls, but they grew with no particular orientation.

Figure 3. Morphology of regenerating axons. Immunostaining was performed using an antibody against neurofilament-M. Axons were detected using epi-fluorescence

microscopy. **(Top)** Axons within unmodified SCPs demonstrated relatively little branching. **(Middle)** Axons within FGF-2-modifed SCPs had a more complex morphology, with abundant branching. The boxed area is enlarged **(bottom)** to highlight the ramified structure.

Figure 4. Boutons en passant. Immunostaining was performed using antibodies against neurofilament-M (red) and CGRP (green). Axons were detected using epi-fluorescence microscopy. CGRP-labeled axons within unmodified **(top)** and FGF-2-modified **(bottom)** SCPs demonstrated localized swellings along their length arrows) that were characteristic of boutons en passant. The nanofibrillar layers in the bottom panel autofluoresced green. Scale bar, 25 mm.

Figure 5. Hindlimb functional assessment with the BBB locomotor rating scale. Curves represent the mean +/- the standard error of the mean (n = 5 rats per group). Animals were tested daily for 3 weeks. Rats that received an FGF-2-modified SCP **(black circles)** showed enhanced functional recovery in comparison to rats that received an unmodified SCP **(white circles)**. Single asterisks denote significant differences between the two groups at each time point with $p < 0.05$; double asterisks denote significant differences with $p < 0.01$ (Student's T-test).

Figure 6. Evidence for buildup of pressure within the SCP. Rostral is to the left. Immunostaining was performed using an antibody against neurofilament-M. Axons

within an unmodified SCP were detected using epi-fluorescence microscopy. A large cavity suggestive of a fluid-filled cyst was observed at the caudal end of the device.

Figure 7. Re-vascularization within an FGF-2-modified SCP. Rostral is to the left. Immunostaining was performed using an antibody against collagen IV. Blood vessels (BV) and Schwann cells (SC) were detected within an FGF-2-modified SCP using epi-fluorescence microscopy. Blood vessels and Schwann cells appeared to grow both on the surface of the nanofibrillar layers (right-hand arrows) and in the agarose in between the layers (left-hand arrows).

Figure 8. Exclusion of reactive astrocytes by SCPs. Rostral is to the left. Immunostaining was performed using an antibody against GFAP 3 weeks after injury. GFAP-labeled astrocytes were detected using epi-fluorescence microscopy. The lesion edge is marked with asterisks. Non-reactive astrocytes were observed within the spinal cord tissue distal to unmodified **(left)** and FGF-2-modified **(middle)** SCPs but were largely absent from the SCPs themselves. No glial scarring was observed. In contrast, reactive astrocytes were observed migrating from the lesion edge **(right)** into the lesion center.